Application Project: Final Report

ME-450-001

Sean McGee

April 24, 2021

NORTHERN ARIZONA UNIVERSITY

College of Engineering, Informatics, and Applied Sciences

TABLE OF CONTENTS

DISCLAIMER

This report was prepared by students as part of a university course requirement. While considerable effort has been put into the project, it is not the work of licensed engineers and has not undergone the extensive verification that is common in the profession. The information, data, conclusions, and content of this report should not be relied on or utilized without thorough, independent testing and verification. University faculty members may have been associated with this project as advisors, sponsors, or course instructors, but as such they are not responsible for the accuracy of results or conclusions.

ACKNOWLEDGEMENTS:

This ME-450 project is being submitted by the author (Sean McGee) as a team of one. However, the experiment, results, and documents generated for the ME-495 design experiment which serves as the basis for this report were created as a team of four students: Sean McGee, Skyler Penny, Connor Schmerfeld, and Zachary Small [1]. These other students, while not officially included in the team for this ME-450 project, were instrumental in the completion of this project and their contributions should not go uncredited. Without their help, suggestions, and hard work, this project would almost certainly have been impossible.

INTRODUCTION

This project follows the Thermal Fluid Final Project Design Experiment track. The objective is to assess the accuracy of a MATLAB thermal simulation compared to real-world experimental data. A heat sink was purchased and outfitted with numerous thermocouples spaced over both the base and fins. The heat sink was then placed on a hotplate and allowed to reach thermal equilibrium. Temperature readings were collected from the thermocouples at a sampling rate of 10 Hz for 24 seconds. The heat sink geometry was then imported into a thermal model using MATLAB's PDE Toolbox. Boundary conditions are calculated and applied to the model, and the model is solved numerically. These results will then be compared to experimental data to identify any discrepancies.

The accuracy of the simulation depends largely on the precision with which boundary condition values can be measured or predicted—without a method of accurately determining fluid velocity, turbulence introduced by surface perturbations, and heat transfer coefficient, these factors must be approximated, introducing significant uncertainty. Measuring these values precisely during experimental procedures, while difficult, should produce results with exceedingly little deviation from experimental data. However, in practice, such simulations are typically performed in lieu of potentially costly experiments. In these cases, environmental factors are not known a priori and must be estimated from known values. By estimating these values for this experimental setup using the information available, the simulated results should indicate the approximate accuracy that can be expected from this type of "semi-informed" simulation.

EXPERIMENTAL SETUP

Heat Sink Selection

A suitable heat sink must provide large enough fins to generate a measurable temperature gradient, and sufficient fin spacing to permit thermocouple installation. After weighing several different options, the heat sink shown in Figure 1 was selected and purchased from HeatsinkUSA [2] at a length of 5 inches. This heat sink is manufactured from extruded 6063-T6 aluminum, which exhibits a higher thermal conductivity than most other aluminum alloys [3, p. 373]. This facilitates efficient heat transfer away from the base of the heat sink which is beneficial in typical use cases. For the purposes of this experiment, this high thermal conductivity reduces the maximum temperature difference over the heat sink. A lower thermal conductivity would perhaps make for more interesting results, but investigation of the accuracy of the thermal simulation should be unhindered.

The heatsink has a total of 13 fins which span the length of the base. To simplify communication for the remainder of this report, the center fin will henceforth be referred to as “Fin 1,” and every-other subsequent fin will be numbered increasing toward the edge of the heat sink with Fin 4 being the outermost fin.

Thermocouple Installation

A total of 10 K-type thermocouple were installed at various locations along the surface of the heat sink. These thermocouple sites span only one-quarter of the heat sink because it is assumed that the temperature response of the heat sink will be symmetrical from front-to-back and from left-to-right. Due to the small expected temperature gradient across the heat sink as described previously, minor deviations from this symmetrical behavior are expected to be negligible. Additionally, thermocouples are installed only on every-other fin due to the supposed low temperature difference between adjacent fins.

Installation of additional thermocouples was considered due to the obvious benefits: additional data would more clearly illustrate outliers and erroneous readings, and more comprehensive coverage over the surface of the heatsink would provide more points of comparison between experimental and simulated results. However, these additional thermocouples may also introduce new, different obstacles. Critically, the increased thermal mass of the heat sink and additional obstructions to airflow into the spaces between fins would prove difficult to accurately model for the simulation, and the increased setup time and complexity may hinder the ability to collect data within the allotted timeframe. Instead, it was supposed that ten thermocouples would provide sufficient data while interfering with the natural behavior of the heat sink as little as possible.

Eight thermocouples were installed in pairs across four heat sink fins as shown in Figure 2. Thermocouple sites along the top edges of the fins will henceforth be referred to as “center” sites while sites near the heat sink base will be referred to as “edge” sites. Additionally, two small channels (approximately 1mm wide, 1 mm deep, and 5 mm long) were engraved in opposite corners of the bottom of the heat sink base, and the welded thermocouple junctions were inserted into these grooves. These thermocouple sites will be referred to as Base 1 (along the front edge of the heat sink, opposite from Fin 4 Edge) and Base 2 (diagonally opposed to Base 1). Lastly, one additional thermocouple is placed away from the experimental setup which measures ambient air temperature.

Fin thermocouples were expected to be adhered to the fin surface using thermal potting compound, which was expected to form a mechanically robust joint while introducing small additional thermal mass. This method was unfortunately prevented due to delayed shipment of the potting compound, which forced the use of an improvised solution. Aluminum ducting tape was instead used to adhere the thermocouples to the fin surfaces. Despite its apparently strong adhesive, the tape provided a poor mechanical bond to the fin surfaces, requiring very delicate handling of thermocouples to prevent separation from the heat sink.

This proved tedious to perform, as evidenced by the seemingly haphazard application of aluminum tape shown in Figure 3 (which, despite appearing hastily assembled, was the result of over an hour of careful work!). It is suspected that a thin film of oil persisted on the surfaces of the heat sink from its manufacturing processes which prevented sufficient tape adhesion. Future work of a similar nature should make efforts to thoroughly clean oil from the heat sink in addition to mounting thermocouples using proper thermal potting compound as opposed to aluminum tape.

Forced-Air Barrier

Once the thermocouples were successfully installed, the heat sink was placed on the hotplate and a barrier was erected around the setup as shown in Figure 5. This barrier is made of 1/8-inch-thick hardboard with 1-1/2 inch holes drilled at various locations around its base. The barrier was intended to reduce the effects of seemingly minor air currents in the lab room, which were found to have a profound impact on convective heat transfer in a prior experiment [4]. The holes around the base of the barrier should allow air to be drawn in as needed to replenish air exiting the open top of the barrier due to advection while also restricting the interaction of forced air currents with the experimental setup. However, the frequency of adjustments needed to the experimental setup caused by poor thermocouple adhesion required the removal of one of the four barrier panels. This reduces the effectiveness of the remining three panels but may have had an unintentional positive side effect. In a discussion of the experimental procedure and outcomes with Dr. David Willy, it was suggested that the enclosure formed by all four barrier panels may have caused the internal airflow upwards through the barrier to behave as channel flow [5]. This may cause results to differ from those expected from purely free convection. The incidental removal of one barrier panel may have reduced this effect, although it is not immediately clear to what degree nor how significantly this effect would have impacted experimental results with all four panels installed.

Data Collection

Thermocouples were connected to an NI-9213 module. This module communicates with a LabVIEW VI which collects data from each thermocouple at a sampling rate of 10 Hz. Thermocouple output voltages were converted to temperature readings using a calibration determined in a prior experiment [6], resulting in the calibration curve shown in Figure 6. Data was collected over a span of 24 seconds, producing a total of 240 data points for each of the 11 thermocouples. A sample of data collected is shown in Table 1, and the full table of collected data has been submitted alongside this report as an Excel workbook. This data is shown plotted against time in Figure 7. Finally, the averages and standard deviations for data from all thermocouples are shown in Table 2.

SIMULATION

The heat sink geometry is created in SolidWorks and exported as an STL file. This file can then be imported into MATLAB for simulation using the PDE Toolbox [7]. The geometry is meshed automatically with a specified maximum edge length of 5 mm, producing the mesh shown in Figure 8. MATLAB reports good resulting overall mesh geometry. The mesh is then imported into a thermal model, at which point the remainder of simulation values can be incorporated into the model.

Boundary Conditions

The model is assigned a thermal conductivity k of 200 $^{W}/_{mK}$, approximately equal to that of the heat sink used in the experimental procedures [6, 7]. Ambient air is assumed to have a temperature of about 293 K, Prandtl number *Pr* of 0.69, *k* of 0.03 $^{W}/_{mK}$, and kinematic viscosity ν of 24×10^{-6} $^{W}/_{mK}$ [8, p. 911]. The bottom surface of the heat sink is assumed to be isothermal and about 365 K.

Prediction of Heat Transfer Coefficient h

The above boundary condition values are known to a relatively high degree of certainty. However, calculation of heat transfer through convection relies on identifying the convective heat transfer coefficient *h* of the various heat sink surfaces. This is a nontrivial process as there are several complicating factors. Firstly, the high thermal conductivity of the heat sink compared to the low thermal conductivity of the surrounding air suggests that the temperature gradient over the heat sink should be small. This is corroborated by experimental results, showing a maximum temperature difference of under 10 K. As such, simulations are expected to be sensitive to even small changes in *h*. Secondly, air moving between heat sink fins does not follow a linear path. Consider the simple control volume shown in Figure 9. As air between fins is heated, it will exit the control volume vertically through surface A due to advection. Maintaining conservation of mass requires that additional air must be drawn into the gaps between fins. The majority of this air is assumed to enter through surfaces B and C, as air moving parallel to the fins experiences less resistance to flow compared to air moving perpendicularly to the fins (as would be the case for air entering through surface D). This air, then, is drawn into the control volume horizontally, gets heated by the heat sink, and exits the control volume vertically. The diagram in Figure 10 shows the approximate expected path followed by the air as it undergoes this process. It is important to note that these streamlines are not derived from experimentation or from an academically rigorous source, but rather from simple inspection and reasoning. As such, this is simply hypothesized behavior used here in the absence of a more informed solution.

Nusselt number correlations have been derived for many simple geometries, but none examined over the (admittedly brief) course of this experiment appear to fully encapsulate the expected airflow described above. Perhaps the most obvious such example is that for free convection between two vertical plates [8, p. 566]. While Bergman et al states, “The plates could constitute a fun array used to enhance free convection heat transfer from a base surface…,” diagrams illustrating the applications of this correlation invariably show air being drawn into the channel *vertically* from the bottom edges of the plates. This is shown in Figure 11, for which the source’s caption reads, “Free convection flow between hot parallel plates with *opposite ends* exposed to a quiescent fluid” [8, pp. 564, emphasis added]. It is unclear if this correlation is accommodating of flow entering the channel *horizontally* as is the expected behavior of the heat sink examined here. Other correlations are accompanied by similar qualifications, which at least allude to (or, at most, explicitly state) restrictions which are incompatible with the application in question.

Approximating airflow over the heat sink fins as parallel flow over a flat plate appears to be the simplest appropriate correlation which does not seemingly (or expressly) exclude the present application. Further

work regarding this experiment would include a more detailed analysis of appropriate *Nu* correlations to quantitatively assess their accuracy to experimental conditions. Without such an analysis, the calculation of *h* performed herein is necessarily imprecise. This leads to uncertainties which are likely overestimated, and surely leave room for improvement. Nonetheless, the remainder of this report will continue by assuming the validity of the correlation for parallel flow over a flat plate:

$$h_x = \frac{k}{L_{path}} \cdot 0.332\, Re_x^{1/2}\, Pr^{1/3} \tag{1}$$

The value of *h* for the outermost faces of the geometry is assumed to be approximately 20 $^{W}/_{mK}$, while the bottom surface (which is in contact with the heated surface of the hotplate) is assumed to have negligible heat transfer by convection. The inner faces of the fins experience varying values of *h* depending on the approximate distance air must travel to reach some given location (according to the streamlines shown in Figure 10). This distance is then used as the characteristic length L_{path} in the calculation of both *Nu* and Reynold's number *Re* in order to compute *h* according to Equation 1 above. Additionally, fins farther from the center of the heat sink are expected to experience improved heat transfer characteristics due to greater available airflow. Quantifying this effect appears to require more than simple fluid mechanics equations, likely requiring flow simulations of the experimental setup. This was unable to be completed in the timeframe of this report—instead, the effect will be approximated by assuming increased flow velocity near the outermost fins. This is motivated by the fact that the greater volume of air available to outer fins compared to inner fins is drawn through and equal area, as shown in Figure 12. A cursory examination of expected advection, assuming a 50K temperature increase and a duration of force application of about 1.0 second, reveals an estimated average velocity v_{avg} of:

$$v_{avg} = t \cdot a = t\frac{F}{m} = tg\frac{(\rho_{amb} - \rho_{hot})}{\rho_{amb}} \tag{2}$$

$$v_{avg} \approx 1\text{s} \cdot 9.81\frac{\text{m}}{\text{s}^2} \cdot \frac{\left(1.1614\frac{\text{kg}}{\text{m}^3} - 0.9950\frac{\text{kg}}{\text{m}^3}\right)}{1.1614\frac{\text{kg}}{\text{m}^3}} = 1.41\frac{\text{m}}{\text{s}} \tag{3}$$

It will then be assumed that fins near the edges of the heat sink (e.g., Fin 4) will have a local velocity slightly *higher* than this value, while fins near the center of the heat sink (e.g., Fin 1) will have a local velocity slightly *lower* than this value. Over the approximately 126 mm width of the heat sink, it is assumed the local air velocity at some horizontal distance *x* from the *y*-*z* plane is given by:

$$v_x = 2 - \cos\left(\frac{\pi x}{0.063\text{m}}\right) \tag{4}$$

This corresponds to a maximum velocity of 3.0 m/s at $x = \pm 0.063$ m and a minimum velocity of 1.0 m/s at $x = 0$ m. Much like the streamlines in Figure 10, this equation is not motivated by first principles or by an academic source, but by inspection. More research and analysis may be performed on this topic to develop a more accurate relationship, but this approximation will be assumed sufficient and used for the remainder of this report.

Incorporating the varying flow velocity and characteristic length into Equation 3, values of h were computed over each fin surface. Results are shown in Figure 13. Note that isosurfaces are shown extending through the gaps between fins as well as within the fins themselves purely for ease of visualization—values of *h* are used only for calculation of heat transfer by convection at the surfaces of the fins.

The variation in *h* shown in Figure 13 is qualitatively as anticipated. As mentioned previously, more thorough analysis would be needed to assess how closely these results model actual airflow. While the objective of this project is to assess how closely the simulation can predict experimental behavior (which

will clearly depend on the validity of the boundary conditions applied to the simulation), most applications of such a simulation will likely have similar limitations. Professional deadlines impose the same limits on simulation accuracy that academic deadlines do, in which case the imposed boundary conditions may not ideal representations of actual behavior. Furthermore, even *Nu* correlations applied to ideal use cases can exhibit uncertainty up to and exceeding 25% [8]. While a simulated model may perfectly describe experimental behavior when boundary conditions are known *exactly*, this is virtually never the case. Instead, a more pragmatic assessment may be to investigate how closely the simulation models actual behavior with boundary conditions known *approximately*. It is with this rationalization, along with the results shown in Figure 13, that this report will continue.

Solving the Model

The boundary conditions listed above are applied to the MATLAB thermal model, at which point the solver may begin the required calculations. A solution was reached within about 30 seconds. The resulting finite element temperature values were plotted by imposing a colormap on the surface of the heat sink geometry. This temperature plot is shown in Figure 14.

RESULTS

The simulated temperature distribution follows the general trends expected for the geometry and those shown by the experimental results. However, the simulated results differ from experimental results in a few areas, as seen in Table 3. The simulated values for all four fin edge thermocouple sites are higher than experimental values by about 5-10 K. Fin center temperatures are also generally overestimated by the simulation, with the exception of Fin 1 Center which has a simulated temperature about 2 K lower than the experimental value. Excluding Fin Edge 4 from the data as an outlier, the maximum error of simulated results from experimental data is 9.4%, with an average error of 4.6%.

DISCUSSION

Overall, while the simulated results differ noticeably from experimental results, the results are still quite informative of real-world behavior. The primary limitation is the large uncertainty associated with the results. Reducing this uncertainty would require more information regarding local flow velocity, identifying a more accurate *Nu* correlation, and more precise control over thermocouple adhesion and location. Given these improvements, simulation results may be achieved within about 1 K of experimental values. This error should be negligible for even particularly demanding practical applications of such a simulation. However, even without such improvements, the simulated temperatures produced here deviate from experimental results by a maximum of about 10% relative to ambient temperature. Given the approximations and generalizations made to arrive at these results, their accuracy is remarkable.

CONCLUSIONS

Simulation of the heat sink's steady state thermal response produced encouraging results. Despite an imperfect experimental setup, uncertainty regarding local flow velocity and convective heat transfer coefficient, and difficulty identifying an appropriate Nusselt number correlation, the average deviation of simulated results from experimental data was 5% relative to ambient temperature. This is quite small on the scale of practical engineering simulations, and sufficient to gain meaningful insight into the actual behavior of the heat sink under experimental conditions. If an application demands increased accuracy, several improvements can be made. Identification of an improved Nusselt number correlation can improve the calculation of local heat transfer coefficients. Taking measurements of experimental flow velocity would also contribute to improving these values. Using a more robust adhesive (such as the originally planned thermal potting compound) to mount thermocouples to the surface of the heat sink would lend added confidence to experimental results. Finally, the effectiveness of the air current barrier and the effects of introducing more thermocouples to the surface should be evaluated and quantified to improve the quality of the experimental setup and results as much as possible. However, implementing these improvements is expected to increase the setup time, complexity, and cost of such an experiment. Where the detriments of these issues outweigh the accompanying increase in accuracy, the suitability of a coarser approximation as performed here should not be undervalued.

APPENDICES

Appendix I: Figures

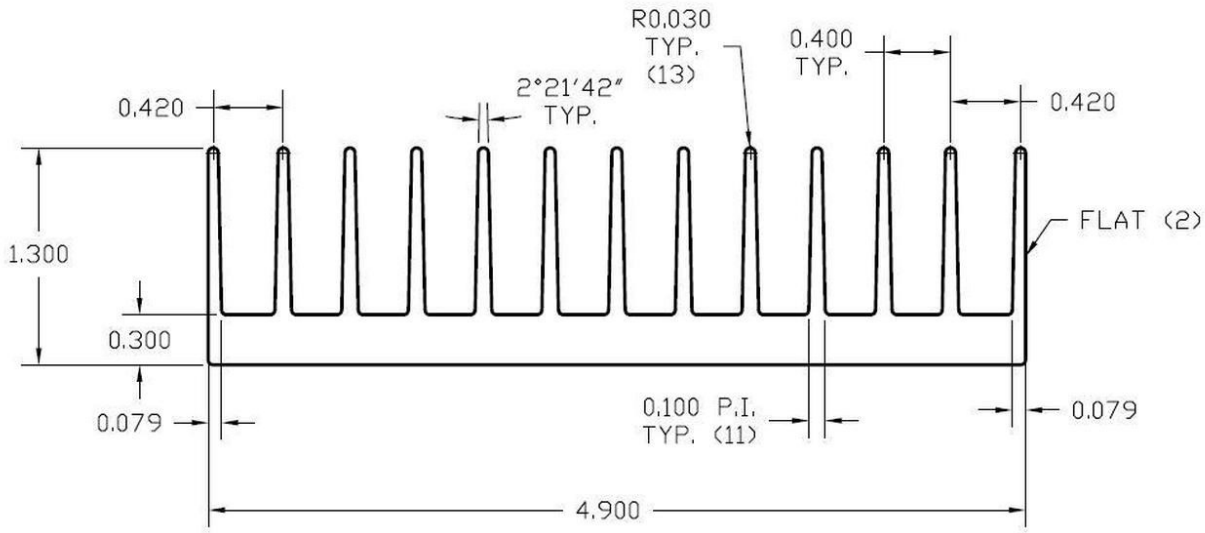

Figure 1: Heat sink cross-section [2]

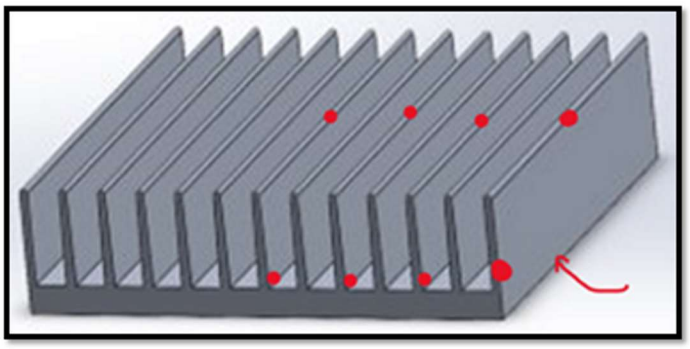

Figure 2: Fin thermocouple locations

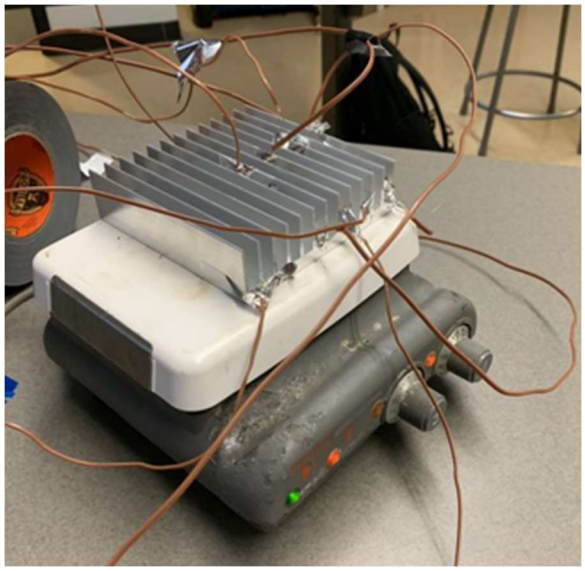

Figure 3: Heat sink with installed thermocouples

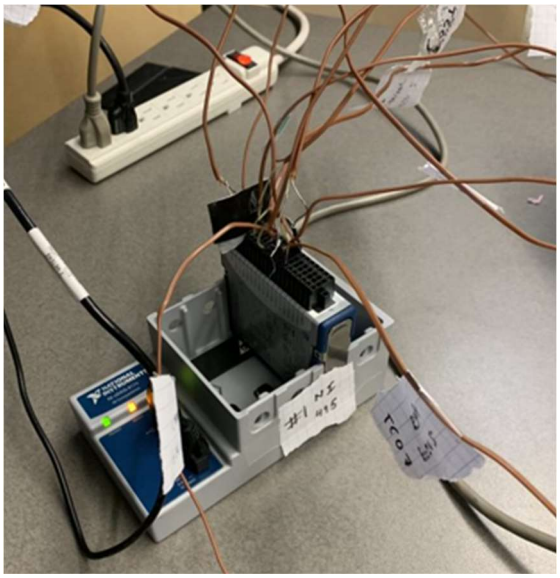

Figure 4: Thermocouples connected to NI-9213 module

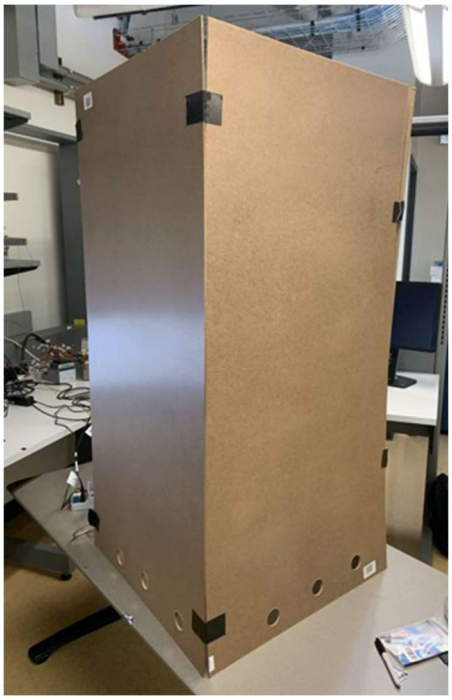

Figure 5: Barrier surrounding experimental setup

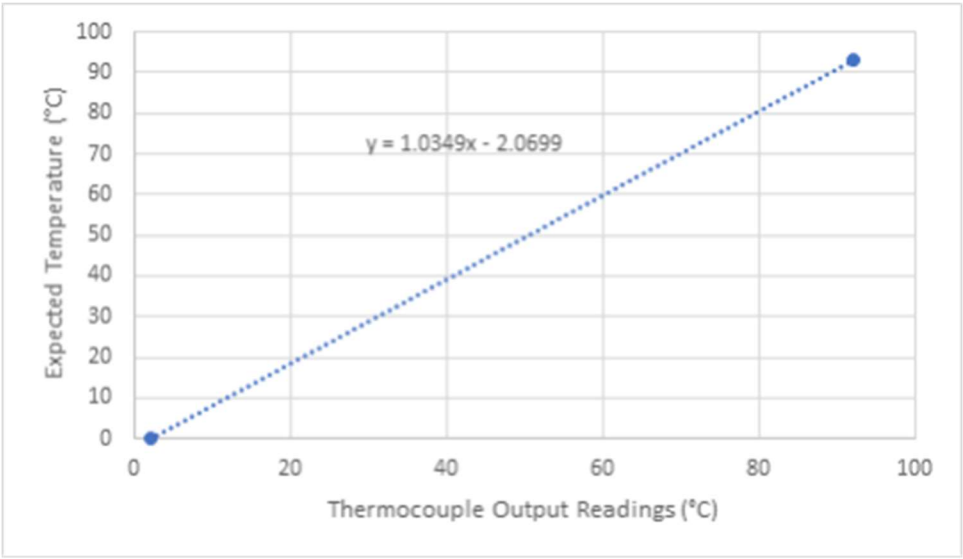

Figure 6: Thermocouple calibration curve

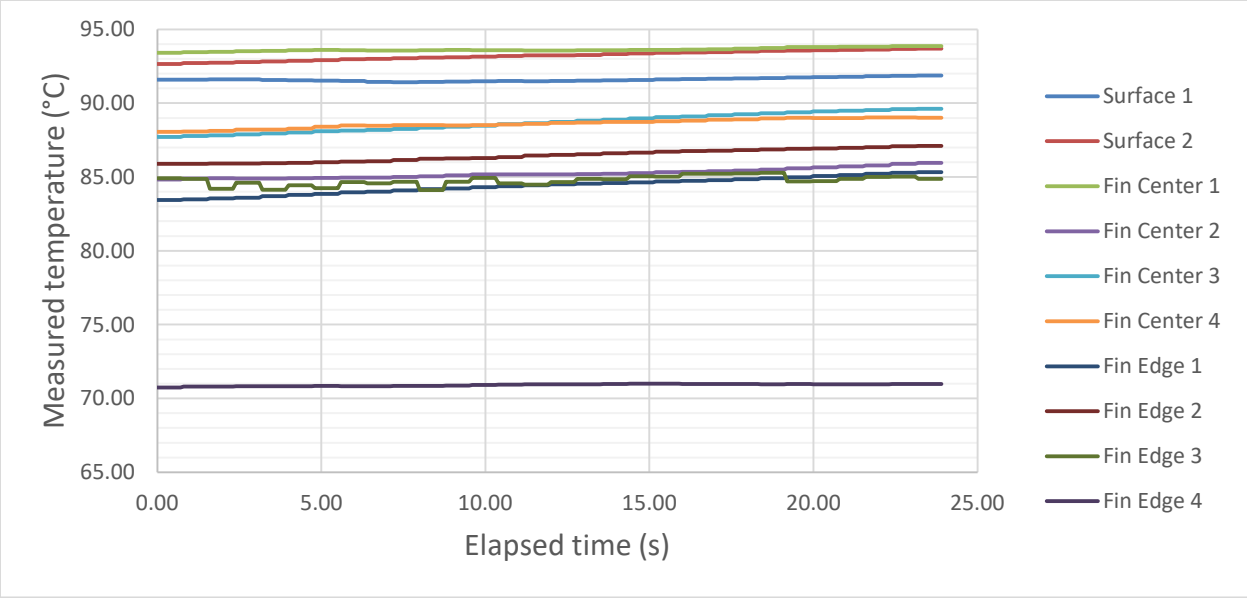

Figure 7: Plot of experimental data over time

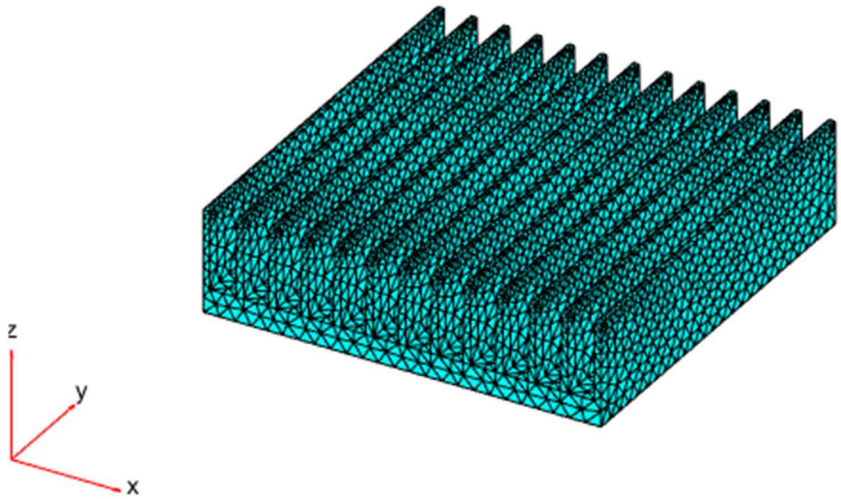

Figure 8: Heat sink geometry meshed in MATLAB

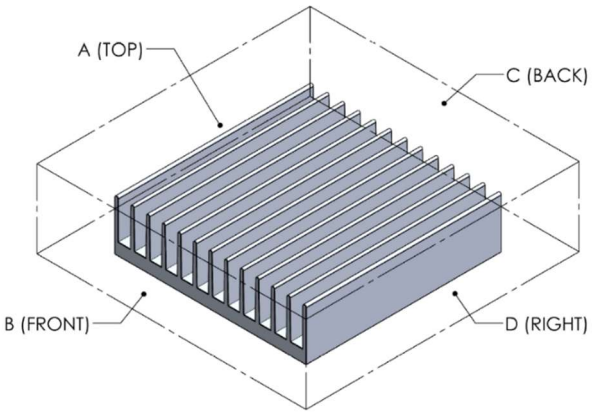

Figure 9: Control volume drawn about heat sink

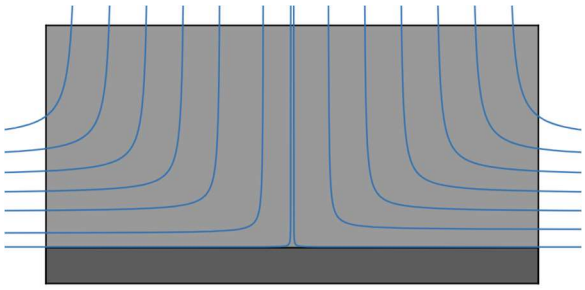

Figure 10: Anticipated airflow between fins

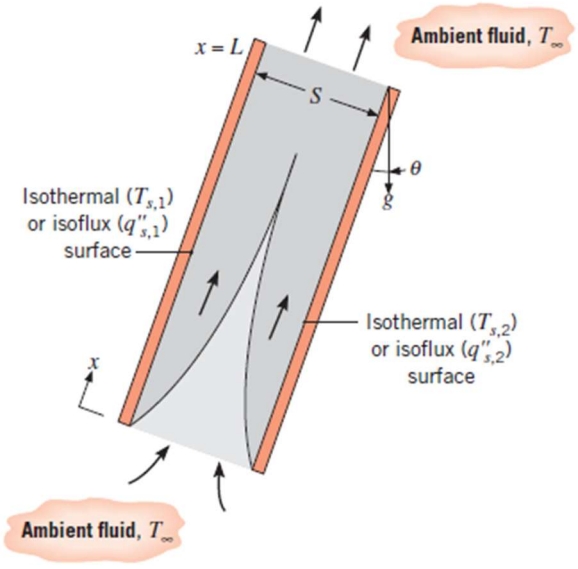

Figure 11: Diagram for free convection between parallel plates [8, p. 564]

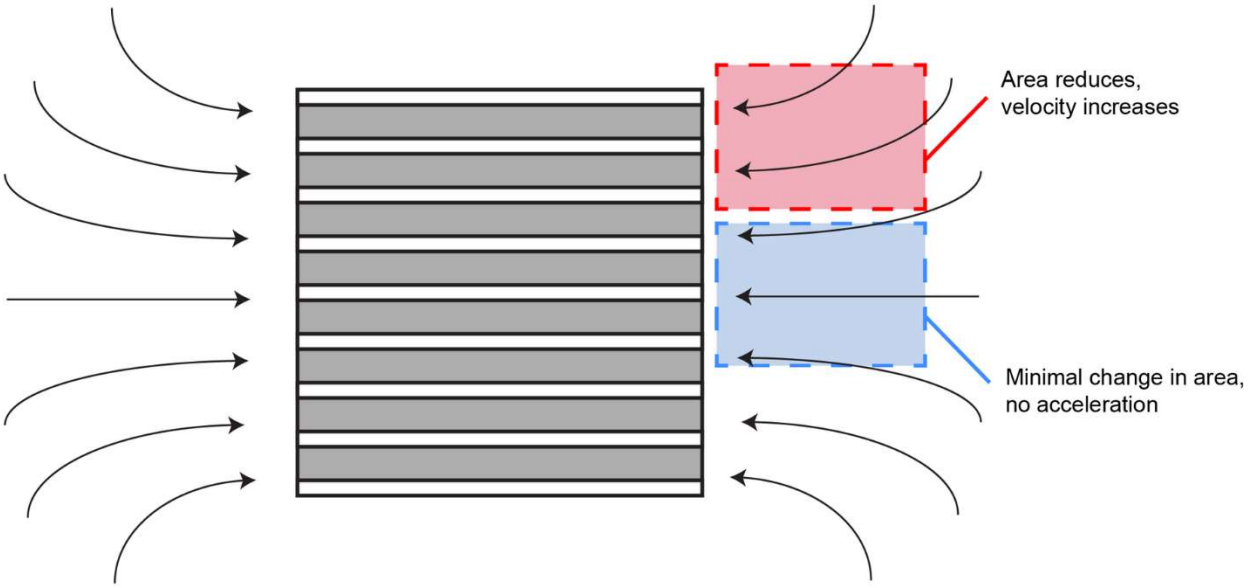

Figure 12: Changing flow velocity entering heat sink [9]

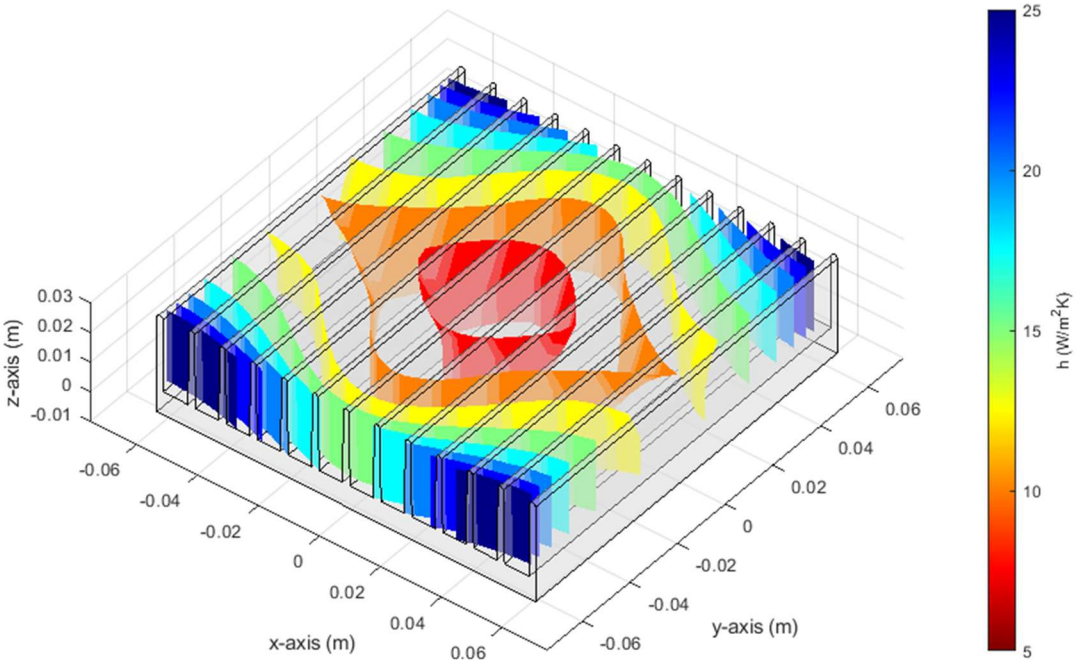

Figure 13: Isosurfaces of calculated h *values*

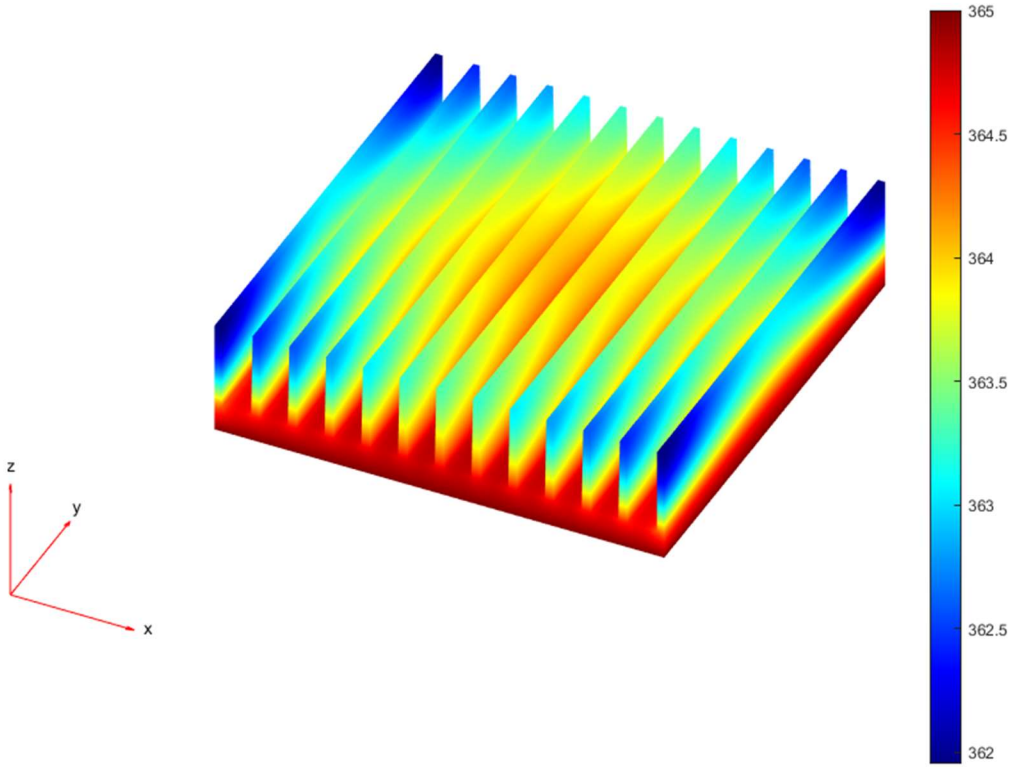

Figure 14: Simulated thermal analysis results (temperatures in K)

Appendix II: Tables

Table 1: Abbreviated experimental results

Elapsed time (s)	Base 1 Temp. (°C)	Base 2 Temp. (°C)	Fin Center 1 Temp. (°C)	Fin Center 2 Temp. (°C)	…	Fin Edge 4 Temp. (°C)	Ambient Temp. (°C)
0.00	91.60	92.66	93.42	84.84	…	70.75	20.10
0.10	91.60	92.66	93.42	84.84	…	70.75	20.10
0.20	91.60	92.66	93.42	84.84	…	70.75	20.10
0.30	91.60	92.66	93.42	84.84	…	70.75	20.10
0.40	91.60	92.66	93.42	84.84	…	70.75	20.10
0.50	91.60	92.66	93.42	84.84	…	70.75	20.10
0.60	91.60	92.66	93.42	84.84	…	70.75	20.10
0.70	91.60	92.66	93.42	84.84	…	70.75	20.10
0.80	91.59	92.71	93.45	84.89	…	70.80	20.10
0.90	91.59	92.71	93.45	84.89	…	70.80	20.10
1.00	91.59	92.71	93.45	84.89	…	70.80	20.10
…	…	…	…	…	…	…	…
23.00	91.85	93.67	93.86	85.88	…	70.98	20.21
23.10	91.85	93.67	93.86	85.88	…	70.98	20.21
23.20	91.88	93.71	93.88	85.96	…	70.98	20.22
23.30	91.88	93.71	93.88	85.96	…	70.98	20.22
23.40	91.88	93.71	93.88	85.96	…	70.98	20.22
23.50	91.88	93.71	93.88	85.96	…	70.98	20.22
23.60	91.88	93.71	93.88	85.96	…	70.98	20.22
23.70	91.88	93.71	93.88	85.96	…	70.98	20.22
23.80	91.88	93.71	93.88	85.96	…	70.98	20.22
23.90	91.88	93.71	93.88	85.96	…	70.98	20.22

Table 2: Average experimental values

Thermocouple Location		Average Temp. (K)	Std. Dev. (K)
Fin 1	Center	366.8	0.12
	Edge	357.6	0.56
Fin 2	Center	358.4	0.32
	Edge	359.6	0.41
Fin 3	Center	361.8	0.61
	Edge	357.9	0.32
Fin 4	Center	361.8	0.30
	Edge	344.1 *	0.07
Base 1		364.8	0.12
Base 2		366.4	0.31
Ambient		293.1	0.03

*(Note: Fin 4 Edge, marked by *, is an outlier and will be excluded from further analysis)*

Table 3: Comparison of simulated and experimental results

Thermocouple Location		Simulated Temp. (K)	Exp. Temp. (K)	% Diff. from Amb.
Fin 1	Center	364.0	366.8	3.9%
	Edge	364.3	357.6	-9.4%
Fin 2	Center	363.8	358.4	-7.6%
	Edge	364.2	359.6	-6.5%
Fin 3	Center	363.5	361.8	-2.4%
	Edge	364.0	357.9	-8.6%
Fin 4	Center	363.0	361.8	-1.7%
	Edge	363.8	344.1	-27.8%
			Average error:	**-4.6%**

Appendix III: References

[1] S. McGee, S. Penny, C. Schmerfeld and Z. Small, "Heat Sink Model Validation," Flagstaff, 2021.

[2] HeatsinkUSA, "4.900" Wide Extruded Aluminum Heatsink," 2021. [Online]. Available: https://www.heatsinkusa.com/4-900-wide-extruded-aluminum-heatsink/. [Accessed 23 04 2021].

[3] E. Oberg, F. Jones, H. Horton, H. Ryffel and C. McCauley, Machinery's Handbook, 31 ed., South Norwalk, CT: Industrial Press, Inc., 2020.

[4] Northern Arizona University, *Experimental Validation... for an Extended Fin - ME-495,* Flagstaff, AZ, 2020.

[5] D. Willy, Interviewee, *Data Analysis Check Follow-Up.* [Interview]. 20 04 2021.

[6] Northern Arizona University, *Introduction to Data Acquisition ... ME-495,* Flagstaff, AZ, 2021.

[7] MathWorks, "PDE Toolbox - Heat Transfer," 2021. [Online]. Available: https://www.mathworks.com/help/pde/heat-transfer-and-diffusion-equations.html. [Accessed 23 04 2024].

[8] T. L. Bergman and A. S. Lavine, Fundamentals of Heat and Mass Transfer, 8th ed., Hoboken, NJ: John Wiley & Sons, 2017.

[9] M. E. McGee, "Diagram of Changing Flow Velocity," Flagstaff, 2021.

[10] R. S. Figliola and D. E. Beasley, "Uncertainty Analysis," in *Theory and Design for Mechanical Measurements*, 5th ed., Hoboken, NJ: John Wiley and Sons, 2011, pp. 168-176.

[11] MatWeb, "Aluminum 6063-T6," [Online]. Available: http://www.matweb.com/search/datasheet_print.aspx?matguid=333b3a557aeb49b2b17266558e5d0dc0. [Accessed 23 04 2021].